Title: Prediction of the lignocellulosic winery wastes behavior during gasification process in fluidized bed: Experimental and theoretical study

Authors: Rodriguez Rosa, Mazza Germán, Fernandez Anabel, Saffe Alejandra, Echegaray Marcelo

PII: S2213-3437(18)30507-4
DOI: https://doi.org/10.1016/j.jece.2018.08.054
Reference: JECE 2602

To appear in:

Received date: 17-6-2018
Revised date: 16-7-2018
Accepted date: 25-8-2018

Please cite this article as: Rosa R, Germán M, Anabel F, Alejandra S, Marcelo E, Prediction of the lignocellulosic winery wastes behavior during gasification process in fluidized bed: Experimental and theoretical study, *Journal of Environmental Chemical Engineering* (2018), https://doi.org/10.1016/j.jece.2018.08.054

Prediction of the lignocellulosic winery wastes behavior during gasification process in fluidized bed: Experimental and theoretical study

Rodriguez Rosa*, Mazza Germán**, Fernandez Anabel*, Saffe Alejandra*, Echegaray Marcelo*

(*) Instituto de Ingeniería Química - Facultad de Ingeniería (UNSJ) - Grupo Vinculado al PROBIEN (CONICET-UNCo)
(**) Instituto de Investigación y Desarrollo de Procesos, Biotecnología y Energías Alternativas PROBIEN (CONICET-UNCO)

Corresponding autor e-mail and telephone: rrodri@unsj.edu.ar, +54-264-4211700, int. 453

Abstract

This work presents studies about the gasification of the lignocellulosic winery wastes in fluidized bed to obtain energy. Based on the exergy analysis, the exergetic improvement potential (IP) and sustainability index (SI) variations with different operational variables were analyzed. IP increases and SI decreases when moisture content, ER and SBR augment. On the other hand, both indexes present contrary behavior with the temperature increasing.

Additionally, the kinetic behavior was investigated using a macro thermo-balance. The thermal decomposition of the studied biomass wastes at three heating rate, 5, 10 and 15ºC/min under steam/air mixture atmosphere show that the gasification takes place in three visible stage: water vaporization, pyrolysis and the last step associated with the reaction of the char by CO_2. The distributed activation energy model method (DAEM) was used. The decomposition is not a single reaction stage, it includes the contributions of parallel reaction steps on the global reaction rate.

Last, the fluidization was analyzed using air at room temperature and local atmospheric pressure. Each experiment was carried out with 100% and 75% v lignocellulosic wastes. Segregation, slugging and channelization in all studied cases. However, the addition of sand particles improves the behavior of both winery wastes.

Keywords: lignocellulosic winery wastes; fluidized bed; kinetic analysis; exergetic improvement potential; sustainability index; fluidodynamic study.

Introduction

The global energy consumption has importantly augmented in last years due to industrial and economic growth and population increase. Instead, in past decades, fossil fuel reserves are continuously depleting, and they also adversely affect the environment. Due to these concerns, significant efforts are directed globally to search for alternate renewable energy and environment friendly fuel sources. Among lignocellulosic biomass has emerged as an attractive source for producing fuels due to its low cost and abundance. So, thermochemical biomass transformation, particularly gasification, is considered as the most promising technology for a large-scale energy production. Biomass gasification comprises of partial oxidation at high temperature (800 – 1000°C) and successive reduction reactions. This process produces a gas mixture, called syngas, which contains H_2, CO, CO_2, H_2O, CH_4 and higher hydrocarbons (tar). The gasification can be carried out using air, oxygen steam or a mixture of them as the gasifying agents. Usually, an air/steam mixture is used. The oxygen content in this atmosphere is lower at stoichiometric content. The obtained syngas is characterized for the H_2 and CO contents.

Otherwise, different operating variables have a high influence on the gasification behavior: biomass feedstock, temperature (T), equivalence ratio (ER, supply air/stoichiometric air) and supply steam/biomass ratio (SBR) [1]. To evaluate the gasification performance, the exergy analysis can be employed (based on the first and second law of thermodynamic). This analysis permits to identify the inefficiencies and their sources allowing an effective management and optimization of the gasification process [2]. Then, many authors used the exergy analysis as a methodology for evaluating the efficiency and the processes sustainability, considering both the amount and the quality of mass and energy streams simultaneously [3]. For a better analysis, the process efficiency at different operational conditions, diverse indicators have been developed. Osturk et al. [4] used a set of exergetic parameters for assessing environmental impact and sustainability, among which can be mentioned the IP and SI [4]. These parameters have been applied to different processes in others works [5], [6].

On the other hand, the biomass wastes involve an important reactions number and their unknown mechanisms, simple kinetic models cannot describe the global reactions. However, experiences where the loss weight is measured with the temperature variation are an important tool in order to

obtain information on chemical kinetics. It is important to note the scarce information found in the literature about this aspect [7]. Elbager et al. [8] studied the steam gasification reactivity, thermal behavior and activation energies of sugar cane bagasse chars prepared at 500, 800 and 900ºC via thermogravimetric analysis (TGA) under non-isothermal conditions at different heating rates. To estimate the activation energies, these researchers used the Vyazovkin and Ozawa–Flynn–Wall methods. They observed that both methods can be efficiently utilized to predict the experimental data and the reaction mechanism. Yao et al. [9] studied the reactions of biomass char CO_2-gasification within granulated blast furnace slag using TGA. They observed that the nuclei production model fitted accurately the experimental data. The founded activation energy was from 52.75 kJ/mol to 64.42 kJ/mol and was lower with the increase of heating rate and the content of blast furnace slag in the mixture. Huang et al. [10] analyzed the chemical looping gasification as a novel and promising gasification technology because it can produce high quality syngas with low cost. They carried out the thermodynamic analysis to predict the feasibility and limitation of redox reaction and the kinetic model to understand the controlling factors of chemical reaction rate.

Considering the used technology to carry out the gasification process, fluidized-bed reactor has been recognized as one of the most effective reactor to transform the biomass into energy [11]. Oliveira et al. [12] determined the minimum fluidization velocity of binary mixtures using the characteristic diagram of pressure drop in the bed and to develop an experimental correlation for the minimum fluidization velocity of biomass and sand mixtures. These researchers used three types of biomass (sweet sorghum bagasse, waste tobacco and soybean hulls) and four sands with different sizes. The results showed that the fluid dynamic behavior of binary mixtures is directly related to the biomass size and shape. They proposed a correlation to predict the minimum fluidization velocities for mixtures of biomass and sand in fluidized beds. Fotovat et al. [13] investigated bubbling fluidization of a sand fluidized bed with different biomass. They employed the radioactive particle tracking to explore the impact of the particle shape factor on the biomass distribution and velocity profiles. The results showed that spherical biomass particles rise faster and sinks lower than the cylindrical biomass particles; furthermore, bubbles are more prone to break in the presence of biomass particles with lower sphericity. These researchers carried out a three-dimensional numerical simulation via an Euleriann-fluid approach with a good reproducibility.

Considering the foregoing and, the fact that the wine industry is one of the most important in the Cuyo Region, Argentina, generating large volumes of lignocellulosic wastes, in order to extend and improve the basic knowledge on gasification process and based on an exergy analysis of literature [14]. IP and SI indexes variation with different operational variables were studied. On the other hand, this work investigates the solid winery wastes kinetic behavior during this process and the hydrodynamic performance of pure biomass and biomass-sand binary mixtures. The kinetic characterization was carried out using a macro thermo-balance and applying the DAEM model. The fluidization of pure biomass and their mixture with sand was carried out using air at room temperature and local atmospheric pressure. These analysis behavior enables the prediction of the fluidized bed gasifier when the solid waste winery is utilized. Such efforts are expected to lead to a better use of these biomass wastes in gasification process.

1. Materials and methods

1.1. Winery wastes characterization

The raw material used in this work were marc and stalks from wine industry. They are located in San Juan Province - Cuyo Region - Argentina. The weight loss at 105ºC, ash and organic matter content were determined according to ASTM standards (ASTM D3173-87, ASTM D3172-89 (02)). Ultimate analyses on the samples were performed using EuroEA3000 model elemental analyzer. The results are shown in Table 1. To evaluate the biomass high heating value (HHV,MJ/kg), the correlations present by Sheng and Azevedo [15] were used:

$$\mathrm{HHV_{biomass}} = -1.3675 + 0.3137\ \mathrm{C} + 0.7009\ \mathrm{H} + 0.0318\ \mathrm{O^{*}} \quad (1)$$

Where O^{*} is the weight percentage (dry biomass) of O and other elements like S, N, Cl, among others, so O^{*}= 100-C-H-ash. The low heating value (LHV, MJ/kg) was calculated from the HHV and the latent heat of water vaporization. The HHV and LHV values are shown in Table 1 for each studied waste.

The concentration of 28 elements in these wastes were determined using inductively coupled plasma mass spectrometer Shimadzu ICPE 9000. Biowastes samples were digested in a Multiwave Go-Anton Paar microwave digestion system using 0.3 g of sample and 10.2 cm3 of three different acid mixtures added to each teflon vessel in the oven. The vessels were heated at 190ºC for 35 min

three times. Each sample was digested in triplicate. De-ionized water, nitric acid (65%), hydrofluoric acid (47-51%) and hydrogen peroxide (30%) were used throughout the work. The experimental results are shown in Table 2.

The values of lignin, cellulose and hemicellulose contents, expressed in percentage, were determined by ASTM standard (ASTM D1106-56, ASTM D1103-60 and ASTM D1103-60, respectively). These analyses were carried out by the laboratory of the Chemistry Section of Agro Products (EEAOC-Estación Experimental Agroindustrial Obispo Colombres) -Tucumán / Argentina. The analysis results are expressed in dry basis. The results are shown in Table 3.

On the other hand, the samples were sieved to obtain classified particles in diverse ranges. For the mixture experiences, biomass and sand particles were used. The river sand and biomass were sieved to obtain classified particles in different ranges. Tyler Standard Mesh sizes were used for the characterization (ASTM E - 11/95). Sauter diameter ($\overline{Dp}$) represents the material diameter, and it is fixed for the sand (between 0.25mm and 0.71mm). The sieving procedure is used to obtain the particle size distribution (ANSI/ASAE S424.1, 2006) and to categorize the particles according to the Geldart Classification (GC) [16]. The results are shown in Figure 1 and Table 4. $\overline{\mathrm{D}}\mathrm{p}$ is calculated by the following expression:

$$\overline{\mathrm{D}}\mathrm{p} = \left[\sum \frac{\mathrm{Xi}}{\mathrm{dp}}\right]^{-1} \quad (2)$$

Where Xi is the mass fraction of retained particles in the mean diameter interval (dp between two sieves). The determination of the real density of the particles was made liquid pycnometer technique. The experiment was performed in triplicate, using water as fluid. The bulk density determination was carried out following the ASTM Standard Test Method for Bulk Density of Densified Particulate Biomass Fuels E873-82

1.2.Experimental method to carry out the kinetic analysis of winery wastes gasification

The experiments were carried out in a macro thermo-balance (macro-TGA). It is formed by a tubular reactor of 5cm of internal diameter and 100cm of height. It is heated by electrical resistance and is coupled to an analytical balance. This equipment is connected to ~~a~~ control system, through

which it is possible to vary the heating rate and to register time, mass data and temperature in a computer.

Experiments were carried out under air/steam atmosphere, the steam flow rate was 0.17mL/min, guarantying the steam/biomass ratio equal to 2.5 [17]. The temperature increased from ambient temperature (approximately 25ºC) to 900ºC. This final temperature ensures the highest decomposition. Three heating rates, 5, 10 and 15ºC/min were used. In order to minimize heat transfer and mass phenomena, 5g of sample with size between 0.212 and 0.250mm were used. Figure 2 shows the utilized reactor.

1.3.Experimental procedure to study the hydrodynamic behavior of winery wastes

The tests were carried out in a transparent plexiglass cylindrical cold flow fluidized bed with an internal diameter of 0.137 m and a height of 1.7 m fitted with a perforated distributor plate and a stainless-steel mesh of 0.1 mm diameter. Air was used as the fluidizing agent. Experiments were conducted at room temperature and atmospheric pressure. The experimental setup is presented in Figure 3. A Kimo differential pressure transmitter (CP213 B-O) was used to register the pressure. Also, Kimo flowmeter (Function SQRT/3) was used to measure the gas flow rate.

Each experiment was carried out with 100% and 75% v lignocellulosic wastes for two different fixed bed heights (L_{bed}/D_{bed} = 0.50 and L_{bed}/D_{bed} = 0.75). The particles were homogenized and added to the bed until they reached stablished bed height of the respective test. The minimum fluidization velocity has been determined from the plot of bed pressure drop vs. superficial gas mass velocity, increasing and decreasing flow air rates for each studied case. The Umf was estimated through the graphical method [18], as the intersection of the pressure drop line of the fixed bed with that for the fluidization state [19]. The bed height, pressure loss and gas flowrate were registered. Also, each condition was repeated 3 times and each test was filmed so as to analyze the fluidization behavior.

1.4. Exergetic indicators

Echegaray et al. [14] proposed a nonstoichiometric equilibrium model in order to find the composition of syngas and the exergy efficiency (η_{ex}). This model is based on minimizing Gibbs free energy in the system [20]. It is derived from the important chemical reactions that occur during biomass gasification are based on the following assumptions: 1) biomass is represented by the

general formula CH_aO_b. Due to the biomass contains insignificant amount of N y S in comparison to the preceding elements, they are not considered 2) the reactions are at thermodynamic equilibrium (at atmospheric pressure = 1 bar), 3) the reactions proceed adiabatically (heat losses neglected), 4) ash of biomass wastes are not considered, 5) the reactions of heat losses are neglected, 6) no chars living with the exit of the gasifier products.

Taking into account that η_{ex} clearly helps determine efficiency improvements and reductions in thermodynamic losses attributable to a process, IP and SI can be calculated. The environmental impact can be reduced proposing measures to increase exergy efficiency, diminishing the energy losses [21]. It is clear that maximum improvement in the η_{ex} for a process is reached when the lost exergy (ε_L, kJ/h) is minimized. Therefore, different authors proposed the use of this concept to analyze a process [22], [23]. IP is given by:

$$IP = \left(1 - \frac{\eta_{ex}}{100}\right) \varepsilon_L \quad (3)$$

This indicator is used for comparing different conditions of processes, even though the obvious maximum improvement for a given process is its total exergy loss. On the other hand, the exergy analysis results are relative to this environment, generally the actual local environment. This linkage between exergy and the environment has implications regarding the environmental impact. So, it is possible to utilize exergy analysis to assess a system and its environmental impact. For that, the SI is defined as the relation between the input exergy and the exergy losses of the system. This index can get information about the process effect on the environment, and it is considered a significant evaluation parameter [23]. The SI is calculated as:

$$SI = \frac{1}{1 - (\eta_{ex}/100)} \quad (4)$$

Both index, IP and SI, vary with the different operational parameters, such as SBR, ER, T and waste moisture.

1.5. Kinetic analysis. Theory

There are two main mathematical approaches to obtain the kinetics parameters from the thermogravimetric data: model-free (isoconversional) methods and model-based (non-isoconversional) methods [24]. Model-free methods enable determination of kinetic parameters without knowledge of the reaction mechanism [25], while model-based methods allow the determination of the controlling reaction mechanism and reaction order. In this work, DAEM was applied. This method, developed by Vand [26], has been widely utilized for analyzing the complex reactions occurring during the pyrolysis of fossil fuels. This model assumes that number of parallel irreversible first order reactions that have different kinetic parameters occur simultaneously. Apparent activation energy (E), apparent pre-exponential factor (A*)* and f (E) can be calculated by following expression [27]:

$$\ln \beta/T^2 = \ln RA/E + 0.6075 - E/RT \quad (5)$$

Where β is the heating rate and R is the universal gas constant (0.008314 kJ/molK). Eq. (5) develops a linear relationship between $\ln\beta/T^2$ and 1/T with the slope of (-E/R). The E and A can be determined from the slope and intercept of the plots.

2. Results and discussion

2.1. Characterization

Table 1 shows the results obtained by ultimate and proximate analysis for the studied winery wastes. Taking into account the first analysis, the marc has the highest carbon (52.91 %) and hydrogen (5.93 %) contents. Furthermore, the stalk has the highest nitrogen content (6.37 %). The results are in agreement with those of other investigators [27], [28].

The immediate analysis results show the moisture content of analyzed biomass wastes is lower than 10%. According to Mc Kendry [29], the thermal conversion needs low moisture content biomass, generally less than 50%. In order to know the biowastes easiness to be ignited and then gasified, the volatile matter and fixed carbon contents must be known [29]. So, he grape marc present the highest volatile matter content. The ash content can be a problematic aspect in the energetic use of the lignocellulosic biomass. It is significant to note that the presence of alkali metals and chlorine causes the components of the ash melt and volatilize at low temperatures, even

though, their total composition in biomass is usually lower than that of coal. The studied wastes have a low percentage of ash, affecting positively the high heating value (HHV) [30]. The high content of organic matter makes these wastes very suitable for thermal treatment [31]

The concentrations of several elements in the studied biomass are determined. Fe, Cr, Pb, Sn, Mo, Ni, Ag, Ti, V, Mn, Cd, B are not detected. The other elements concentrations are showing in Table 2. Al, Ca, K, Mg, Na and Si are defined as major elements, and As, Ba, Co, Cu, In, Li, P, Sr, Tl and Zn as trace elements. Comparing with the limits of trace element described in the EN ISO 17225:2014 standard, the As contents were higher than stablished limits, for marc and stalk. The Cu content in the tested biomass reached 14.86 mg/kg, exceeding the limit for commercial use but not for the industrial use. The Zn contents are lower than stablished limits, for both lignocellulosic winery wastes.

The trace elements contents in the raw material is important, considering the environmental protection, due to the dust particles have these elements in their surface and, they are discharged to the atmosphere. If the gas cleaning systems of dust have a low efficiency, high heavy metals quantities are emitted. So, according to Wang et al. [32] the elements can be classified in different groups, taking into account their behavior during the thermal process. Group I includes the non-volatile elements as Ba, Cu and Sr. As, Li and Zn belong to the group II (semi-volatile elements). Group III includes volatile elements as In and Tl. According to Cui et al. [33], most trace elements are relatively enriched in the gas stream during the gasification process. They found that Ca, K, Mg and P were adhered to the surface of bed materials and Zn are principally partitioned into the gas stream.

In order to estimate the quantity of emissions related to the quantity of produced energy, an emission factor was used [34]. This factor considers the trace elements content in the biomass wastes and their HHV and it was calculated for the semi-volatile and volatile elements. Table 5 shows the calculated values of this emission factor for As, In, Li, Tl and Zn. The obtained values of this factor are similar for both winery wastes.

Considering the Na and K release during the gasification process, Ftehi et al. [35] concluded that during the pyrolysis stage up to 55% and less than 10% of Na and K, respectively, was released. However, Bartocci et al. [36], observed that the Na release is about 65% of the initial quantity for gasification and, the Ca, Mg and K release is about 45%.

On the other hand, the Na, K, Mg, P and Ca contents in the biomass are very important due to these elements. Their reaction with Si produces an adhesive liquid phase, which can blockage the reactor outputs.

The contents of lignin, hemicellulose and cellulose vary depending on the biomass type; also, for the same biomass type, these contents depend on the environmental conditions of the generation place. Agree to the current literature, the woody vegetable species have strongly bound fibers and they are richer in lignin, however, herbaceous vegetables have more loosely bound fibers, indicating lower lignin content [37]. Considering the obtained results (Table 3), the highest hemicellulose and cellulose contents are present in stalk, 5.78 and 16.02%, respectively. The marc has the highest lignin content, 37.97%. McKendry worked with different biomass and he reported values for cellulose, hemicellulose and lignin equals to 40–50%, 20–40% and 10–40%, respectively [29] and Yang, et al. determined hemicellulose, cellulose and lignin contents about 20–40, 40–60, and 10–25% respectively [38]. Hence, the obtained values are in the order of reported by these authors. Taking into account the lignin content, it is important to note that, during the thermal decomposition of this compound, benzene rings with high stability and high molecular weight compounds are produced, contributing to the char and tar production [39].

2.2. Exergetic Improvement Potential and Sustainability Index

In order to analyze the IP and SI with temperature variation, SBR value was set at 2, ER at 0.25 and the moisture content of the biowastes was equal to 13%. Figure 4 (a) shows this variation for the stalk gasification. Both studied biowastes present similar behavior. The exergetic efficiency increases when the gasifier temperature augments and consequently, SI growths and IP diminishes. These results are similar to those obtained by Zhang et al. [40]. The lower temperatures favor the exothermic reactions of CH_4 and CO_2 formations. On the other hand, the higher temperatures favor the endothermic reactions as the H_2 and CO formation reactions. Therefore, in the product, moles of H_2 and CO increase and consequently the exergy efficiency of the process. So, in the syngas composition, the moles of these gases augment and consequently, exergetic efficiency of the process increases.

To study the ER influence on the IP and SI indexes, the gasifier temperature was set at 850ºC and SBR at 1.5 and the moisture content of the biowastes was equal to 13%. Figure 4 (b) shows that SI value of the stalk gasification diminishes and IP value augments with the ER increasing. Marc

presents analogous comportment. It is due to the O_2 content in the gasifying agent promotes the combustion reactions. During the gasification process, these reactions are not desirable due to, they compete with the reactions to transform the biomass in syngas rich in H_2 and CO contents. Marcs present similar behavior.

Considering the influence of SBR in the IP and SI indexes, this parameter was varied when ER value was equal to 0.25, the gasifier temperature equal to 850ºC and the moisture content of biowastes was equal to 13%. IP softly augments and SI decreases slightly when SBR growths (Figure 5 (a)). This comportment is due to the physical exergy of the steam used as the gasifying agent. There is a necessity of supply energy to the water to transform it in steam. So, physical exergy is related to the syngas sensible heat and this is lost when the gas cools and it influences the exergetic efficiency value. Increasing the SBR value, the water content in the produced gas flow increases and also it contributes to the physical exergy.

The high moisture content affects the chemical reactions in the process. To understand how the gasification responds to variations in biomass moisture content, the process was assessed for a range of biomass moisture fractions. The results are also shown in Figure 5 (b). Both wastes present similar behavior. In this case, the gasification agent was air (SBR = 0), the temperature was equal to 850ºC and ER value equal to 0.25. The effect of moisture content was studied between 0 and 40%. The IP increases and SI decreases with the moisture content augments. In this case, the rate of CO_2 production growths, which itself is an exothermic process. In steam-biomass gasification, the liberated heat is consumed by water evaporation rather by the endothermic CO and H_2 reactions. Thus, the CO concentration decrease significantly and the H_2 concentration increase slightly, and then it decreases, explaining the exergetic efficiency decreased with biomass wastes moisture and consequently, SI and IP diminishes and augments, respectively. On the other hand, moisture content has a negative effect on the chemical and physical exergy.

2.3. Kinetic analysis

The thermal decomposition of the studied biomass wastes at three heating rate, 5, 10 and 15ºC/min under steam/air mixture atmosphere show that the gasification takes place in three well defined stage. Figures 6 and 7 show the weight loss and their derivative TG (DTG) curves.

The first step involves heating and weight loss due to the water vaporization and it is produced between 25 and 200ºC, constituting an around 1.82-2.96% weight loss for all the biomass wastes.

The second step corresponds to pyrolysis namely, the thermal decomposition in the absence of oxygen. During this stage (between 200 and 375ºC), the volatile compounds are released and primary char residue is formed. It can be considered that it constitutes a transition stage with the maximum weight loss and abrupt decomposition reaction. The weight loss of this step is about 58.96-59.30%. The maximum weight loss rate of winery wastes is reached at 173-283ºC, 251-297ºC and 303-324ºC at heating rates equal to 5; 10 and 15ºC/min, respectively. These thermal ranges variation is typical of degradation of lignocellulosic biomass, considering that the cellulose, hemicellulose and lignin are the main components of these biowastes [41].The last step (char gasification) occurs between 375 and 900ºC, its weight loss represents a 15.82-19.28% [42]. The little differences in this temperature range, for winery wastes, can be attributed to composition variation.

Considering the kinetic analysis, the Eq. (5) was used to calculate the values of activation energy at each selected level of conversion rate α from the Arrhenius plot of ln (β/T^2) versus 1/T. The conversions from 0.1 to 0.9 was considered for describing the application of DAEM (Figure 8), it is due to the fact that for higher conversions the plots are nonlinear and show different behavior due to the different chemical reactions occur [27]. The apparent activation energy and pre-exponential factor values are reported in Table 6. The E dependence with α shows that the decomposition is not a single reaction stage but, it includes the contributions of parallel reaction steps on the global reaction rate (Figure 9).

In this way, global kinetic parameters are less useful for studying the thermal degradation of the fuels since particular reactions not can be defined [43]. Nevertheless, this analysis is relevant in order to obtain general tendencies, with particular regard to the assessment of the reactivity of the fuels.

2.4. Flow characteristics of the waste winery-sand mixtures

Figures 10 and 11 show the pressure drop versus air velocity (characteristic curve), to increasing and decreasing flow air rates for each studied case. The average values of this parameter for each biowastes and conditions are shown in Table 7. The Umf value increases with the L_{bed}/D_{bed} augmentation, both for pure biomass particles and for binary mixtures with sand, as predictable, due to the bed weight. This parameter decreases, for the same L_{bed}/D_{bed} ratio, with the sand addition due to the minor diameter of this material, the increasing voidage and the high irregularity of the

biomass particles [12]. These results show that the sand addition leads to an important effect on the bed hydrodynamics. A higher Umf signifies a disadvantage considering the energy consumption. Considering the obtained Umf values for marcs and stalks, for a same biomass/sand ratio, an important difference is not observed due to a compensation of particle diameter, density and voidage effects on the hydrodynamic behavior. For a determined biomass-sand mixture, very small differences were observed considering the L_{bed}/D_{bed} ratio.

Before reaching Umf, the bed pressure drop presents a linear relationship with increasing air velocity. During this stage, the bed height keeps steady without any bed expansion. The obtained curves presented segregation during fluidization, when the air velocity increases, the Umf values are not associated to a single point. This behavior is verified with the high hysteresis, characterized by the differences between the up flow and the down flow curves. This comportment shows that the particles are reorganized during the fluidization process. For gas velocities higher than the minimum fluidization velocities, the growing bubbles in the bed were observed, causing the slugging and channelization, favoring the segregation and producing a large pressure fluctuation [18]. The dissimilarities in density and sizes between the mixture particles produce the segregation in the bed. These phenomena reduce the fluidization quality. Commonly, the sand (higher density) migrates to the bottom of the bed, and the biomass (lower density) migrates to the top. The different shapes of sand and biomass also affects the mixing and segregation performance [44].

Conclusions

This work presents studies on the gasification in fluidized bed of lignocellulosic winery wastes from Cuyo Region (Argentine). Considering the characterization results, it was observed:

- The studied lignocellulosic biowastes have a low percentage of ash, affecting positively the high heating value. The high content of organic matter makes these wastes very suitable for thermal treatment.
- The concentrations of several elements in the studied biomass are determined. Fe, Cr, Pb, Sn, Mo, Ni, Ag, Ti, V, Mn, Cd, B are not detected. The As content in both winery wastes exceeds the limits stablished in the EN ISO 17225:2014 standard and Cu content surpasses the limit for commercial.
- Taking into account the semi-volatile and volatile elements, to estimate the quantity of emissions related to the quantity of produced energy, an emission factor was used. The

obtained values of this factor are similar for both winery wastes. Also, Na, Ca, K and Mg can be released during the gasification process. Further, these elements can react with Si, producing an adhesive liquid phase, which can blockage the reactor outputs.

On the other hand, the exergy analysis allowed to analyze the IP and SI variation with the different operational variables, found the following conclusions:

- SI growths and IP diminishes when the gasifier temperature augments.
- SI value diminishes and IP value augments with the ER increasing.
- IP softly augments and SI decreases slightly when SBR growths.

In consideration of the results of kinetic analysis, it was observed:

- Three stages during thermal decomposition were observed, where the second step called pyrolysis shows the highest weight loss.
- The E dependence with α, for both wastes, shows that the decomposition is not a single reaction stage, but includes the contributions of parallel reaction steps on the global reaction rate.
- The average E value of stalk is higher than these values presented for the marc, however, the difference is not very significant.

Taking into account the fluid-dynamic analysis, the following conclusions were obtained:

- When the biomass is pure, the minimum fluidization velocity (Umf) is higher than this parameter observed for the biomass-san mixtures and, segregation, slugging and channelization in all studied cases.
- The non-desired phenomena are minor when the sand is added. Its addition improves the behavior of both winery wastes. It is important to consider that the heat release during the gasification process could produce differences in the temperature and gas velocity in the bed, varying the fluidization regime in the gasifier.

References

[1] Dhanavath K, Shah K, Bhargava S, Bankupalli S, Parthasarathy R, "Oxygen–steam gasification of karanja press seed cake: Fixed bed experiments, ASPEN Plus process

model development and benchmarking with saw dust, rice husk and sunflower husk", *Journal of Environmental Chemical Engineering,* vol. 6, I. 2, pp. 3061-3069, 2018.

[2] Cohce M, Dincer I,Rosen M, "Energy and exergy analyses of a biomass based hydrogen production system.," *Bioresour. Technol.*, vol. 102, pp. 8466–74, 2011.

[3] Dincer I, Rosen M, Exergy and Energy Analyses, *Environment and Sustainable Development,* 2nd Edition. Elsevier Science, 2013.

[4] Ozturk Murat , Ozek N, Yuksel E, "Gasification of various types of tertiary coals:A sustainability approach," Management, vol. 56, pp. 157–165, 2012.

[5] Aydin H, Turan O, Karakoc T, Midilli A,"Exergo sustainability indicators of a turboprop aircraft for the phases of a flight.," *Energy,* vol. 58, pp. 550–60., 2013.

[6] Aydin H, Turan O, Karakoc TH, Midilli A, "Exergetic sustainability indicators as a tool in commercial aircraft: a case study for a turbofan engine.," *Int. J. Green Energy*, vol. 12, pp. 28–40., 2014.

[7] Rachita Rana R, Nanda S, Kozinski J, Dalay A, "Investigating the applicability of Athabasca bitumen as a feedstock for hydrogen production through catalytic supercritical water gasification", *Journal of Environmental Chemical Engineering,* vol. 6, I1, pp. 182-189, 2018.

[8] Edreis E, Yao H,"Kinetic thermal behaviour and evaluation ofphysical structure of sugar cane bagasse charduring non-isothermal steam gasification.," *J. Mater. Res. Technol.*, vol. 5, no. 4, pp. 317–26., 2016.

[9] Yao X, Yu Q, Wang K, Xie H, Qin Q."Kinetic characterizations of biomass char CO2-gasification reaction within granulated blast furnace slag.," *Int. J. Hidrogen Energy,* vol. 42, no. 32, pp. 20520–8., 2017.

[10] Huang Z, Deng Z, Chen D, He F, Liu S, Zhao K, Wei G, Zheng A, Zhao Z,Li H, "Thermodynamic analysis and kinetic investigations on biomass char chemical looping gasification using Fe-Ni bimetallic oxygen carrier.," *Energy,* vol. 141, pp. 1836–44, 2017.

[11] Faé Gomes G, Philipssen C, Bard E, Zen L, de Souza G, "Rice husk bubbling fluidized bed combustion for amorphous silica synthesis", *Journal of Environmental Chemical Engineering,* vol. 4, I 2, pp. 2278-2290, 2016.

[12] Oliveira J, Cardoso C, Ataíde C, "Bubbling fluidization of biomass and sand binary mixtures: Minimum fluidization velocity and particle segregation," *Chem. Eng. Process.*

Process Intensif., vol. 72, pp. 113–121, 2013.

[13] Fotovat F, Ansart R, iHemati M, Simonin O, Chauki J. "Sand-assisted fluidization of large cylindrical and spherical biomass particles: Experiments and simulation.," *Chem. Eng. Sci.*, vol. 126, pp. 543–59, 2015.

[14] Echegaray E, Castro M, Mazza G, Rodriguez R,"Exergy Analysis of Syngas Production via Biomass Thermal Gasification," *Int. J. Thermodyn.*, vol. 19, no. 3, pp. 178–184, 2016.

[15] Sheng C, Azevedo J, "Estimating the higher heating value of biomass fuels from basic analysis data," *Biomass and Bioenergy*, vol. 28, no. 5, pp. 499–507, 2005.

[16] Kunii D, Levenspiel O. *Fluidization Engineering,Second Edition*, Second. Boston, 1993.

[17] Lim Y, Lee U, "Quasi-equilibrium thermodynamic model with empirical equations for air-steam biomass gasification in fluidized-beds.," *Fuel Process. Technol.*, vol. 128., pp. 199–210, 2014.

[18] Formisani B, Girimonte R, Longo T, "The fluidization process of binary mixtures of solids: Development of the approach based on the fluidization velocity interval," *Powder Technol.*, vol. 185, no. 2, pp. 97–108, 2008.

[19] Rao T,Bheemarasetti J, "Minimum fluidization velocities of mixtures of biomass and sands," *Energy*, vol. 26, pp. 633–644, 2001.

[20] Echegaray E, Rodriguez R, Castro M, "Equilibrium model of the gasification process of agro-industrial wastes for energy production.," *Int. J. Eng. Sc. Innov. Tech.*, vol. 3, p. 6, 2014.

[21] Ahin H, "Exergetic sustainability analysis of LM6000 gas turbine power plant with steam cycle.," *Energy*, vol. 57, pp. 766–774, 2013.

[22] Khanali M, Aghbashlo M,Rafiee S, Jafari A, "Exergetic performance assessment of plug flow fluidised bed drying process of rough rice.," *Int. J. Exergy*, vol. 13, pp. 387–408., 2013.

[23] Anca-Couce A, Berger A, Zobel N, "How to determine consistent biomass pyrolysis kinetics in a parallel reaction scheme," *Fuel*, vol. 123, pp. 230–240, 2014.

[25] Ceylan S, Topçu Y, Pyrolysis kinetics of hazelnut husk using thermogravimetric analysis.," *Bioresour. Tech*, vol. 156, pp. 182–8., 2014.

[26] Vand V, "A theory of the irreversible electrical resistance changes of metallic films evaporated in vacuum," *Proc. Phys. Soc.*, vol. 55, no. 3, p. 222, 1943.

[27] Bhavanam A, Sastry R, "Kinetic study of solid waste pyrolysis using distributed activation

energy model," *Bioresour. Technol.*, vol. 178, pp. 126–131, 2015.

[28] Valente M, Brillard C, Schönnenbeck C, Brilhac F, "Investigation of grape marc combustion using thermogravimetric analysis. Kinetic modeling using an extended independent parallel reaction (EIPR)," *Fuel Process. Technol.*, vol. 131, pp. 297–303, 2015.

[29] Fernandez A, Mazza G, Rodriguez R, "Thermal decomposition under oxidative atmosphere of lignocellulosic wastes: Different kinetic methods application", *Journal of Environmental Chemical Engineering*, vol. 6, I 1, pp.404-415.

[30] Fernández J, Gutierrez F, Del Rio P, San Miguel G, Bahillo A, Sanchez J, Ballesteros M, "Tecnologías para el uso y transformación de biomasa energética," *Madrid: Ediciones Mundi-Prensa*, 2015.

[31] Demirbas A, "Effects of temperature and particle size on bio-charyield from pyrolysis of agricultural residues," *J. Anal. Appl. Pyrolysis*, vol. 72, pp. 243–248, 2004.

[32] Wang Y, Tang Y, Liu S, Wang Y, Finkelman R, Wang B, Guo X ,"Behavior of trace elements and mineral transformations in the super-high organic sulfur Ganhe coal during gasification," *Fuel Process. Technol.*, vol. 177, pp. 140–151, 2018.

[33] Cui H, Turn S, Keffer V, Evans D, Tran T, Foley M, "Study on the fate of metal elements from biomass in a bench-scale fluidized bed gasifier Author links open overlay panel," *Fuel*, vol. 108, pp. 1–12, 2013.

[34] Konieczyńskiego J, *The properties of the emitted respirable dust from selected installations*, in works & studies prace i studia, Polish, 2010.

[35] Fatehi H, Li Z, Bai X, Aldén M, "Modeling of alkali metal release during biomass pyrolysis.," *Proc. Combust. Inst.*, vol. 36, p. 2243–51, 2017.

[36] Bartocci P, Barbanera M, D'Amico M, Laranci P, Cavalaglio G, Gelosia M, Ingles D, Bidini G, Buratti C, Cotana F, "Thermal degradation of driftwood: Determination of the concentration of sodium, calcium, magnesium, chlorine and sulfur containing compounds.," *Waste Manag.*, vol. 60, p. 151–7, 2017.

[37] Stefanidis S, Kalogiannis K, Iliopoulou E, Michailof C, Pilavachi P, Lappas A, "A study of lignocellulosic biomass pyrolysis via the pyrolysis of cellulose, hemicellulose and lignin," *J. Anal. Appl. Pyrolysis*, vol. 105, pp. 143–150, 2014.

[38] Yang H, Yan R, Chen H,Lee D, Zheng C, "Characteristics of hemicellulose, cellulose and lignin pyrolysis," *Fuel*, vol. 86, no. 12–13, pp. 1781–1788,. 2007.

[39] Vassilev V, Baxter D, Andersen L, Vassileva C, Morgan T, "An overview of the organic and inorganic phase composition of biomass," *Fuel*, vol. 94, pp. 1–33, 2012.

[40] Zhang L, Xu C, Champagne P, "Overview of recent advances in thermo-chemical conversion of biomass," *Energy Convers. Manag.*, vol. 51, no. 5, pp. 969–982, 2010.

[41] Burnham A, Dinh L,"A comparison of isoconversional and model-fitting approaches to kinetic parameter estimation and application predictions.," *J. Therm. Anal. Calorim.*, vol 89, pp. 479–490, 2007.

[42] Chen J, Mu L, Jiang B, Yin H, Song X, Li A, "TG/DSC-FTIR and Py-GC investigation on pyrolysis characteristics of petrochemical wastewater sludge," *Bioresour. Technol.*, vol. 192, pp. 1–10, 2015.

[43] Aboyade A, Hugo T, Carrier M, Meyer E, Stahl R, Knoetze J, "Non-isothermal kinetic analysis of the devolatilization of corn cobs and sugar cane bagasse in an inert atmosphere," *Thermochim. Acta*, vol. 517, pp. 81–9., 2011.

[44] Escudié R, Epstein N, Grace J, Bi H, "Effect of particle shape on liquid-fluidized beds of binary (and ternary) solids mixtures: segregation vs. mixing," *Chem. Eng. Sci.*, vol. 61, no. 5, pp. 1528–1539, 2006.

Figure captions

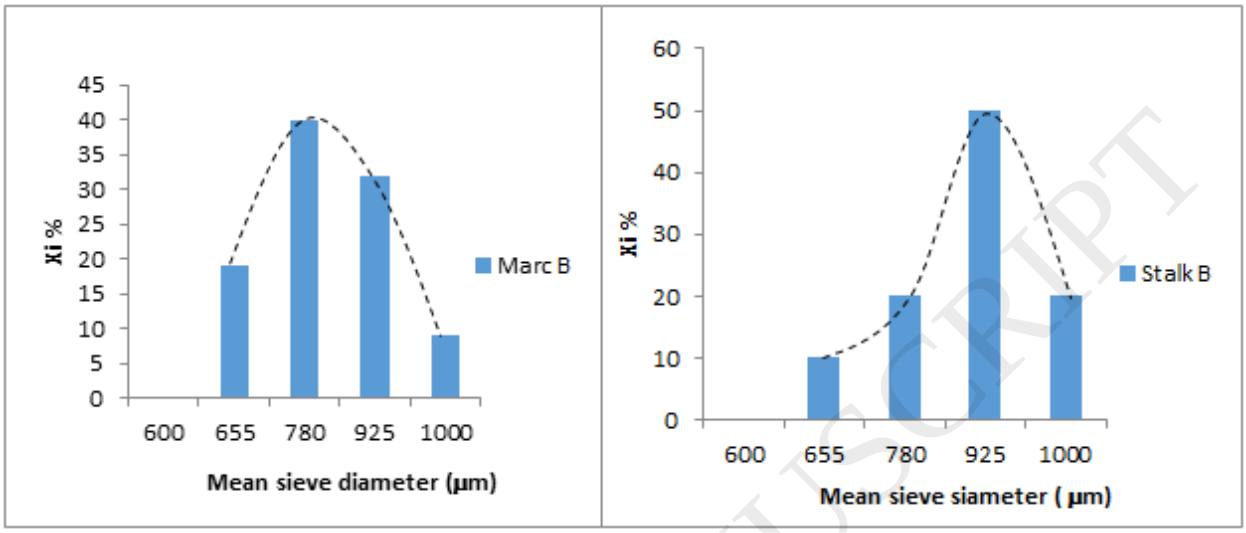

Figure 1. Particle size distribution of the considered biomass particles.

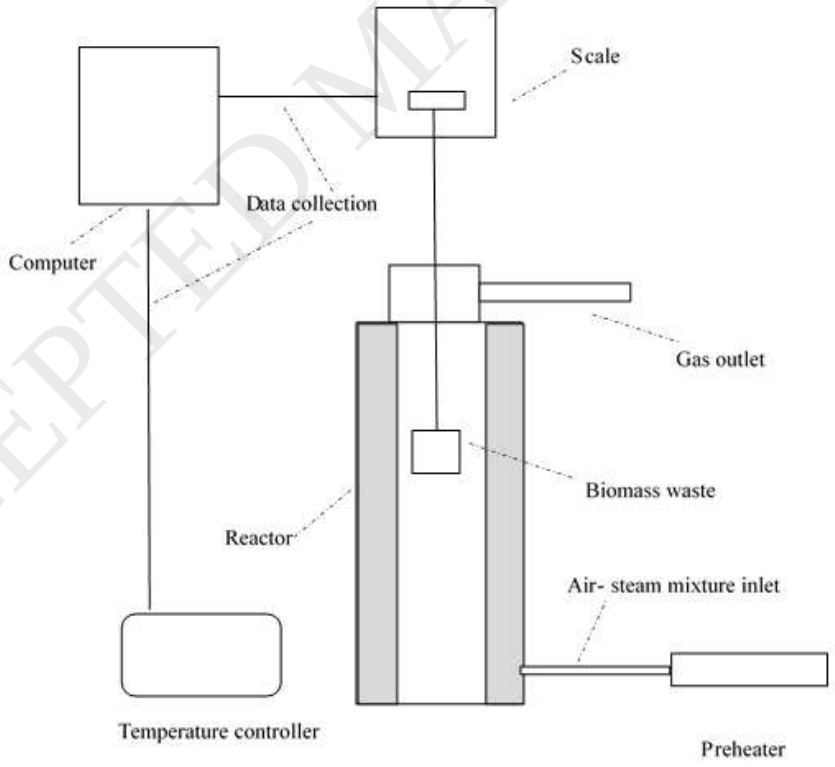

Figure 2. Graphic of weight loss equipment used.

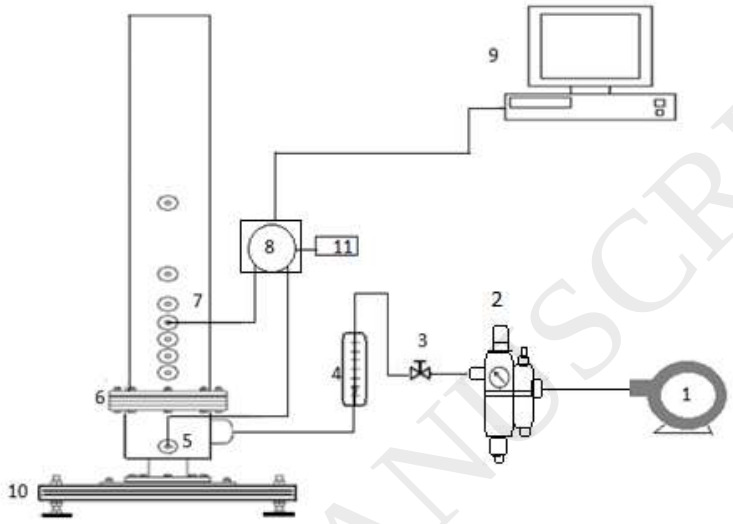

Figure 3. Schematic diagram of the fluidized bed experimental setup. (1) Compressor, (2) filter-regulator, (3) needle valve, (4) rotameter, (5) plenum, (6) distributor plate, (7) biomass particle bed, (8) pressure sensors, (9) data acquisition computer, (10) bed support and (11) power supply.

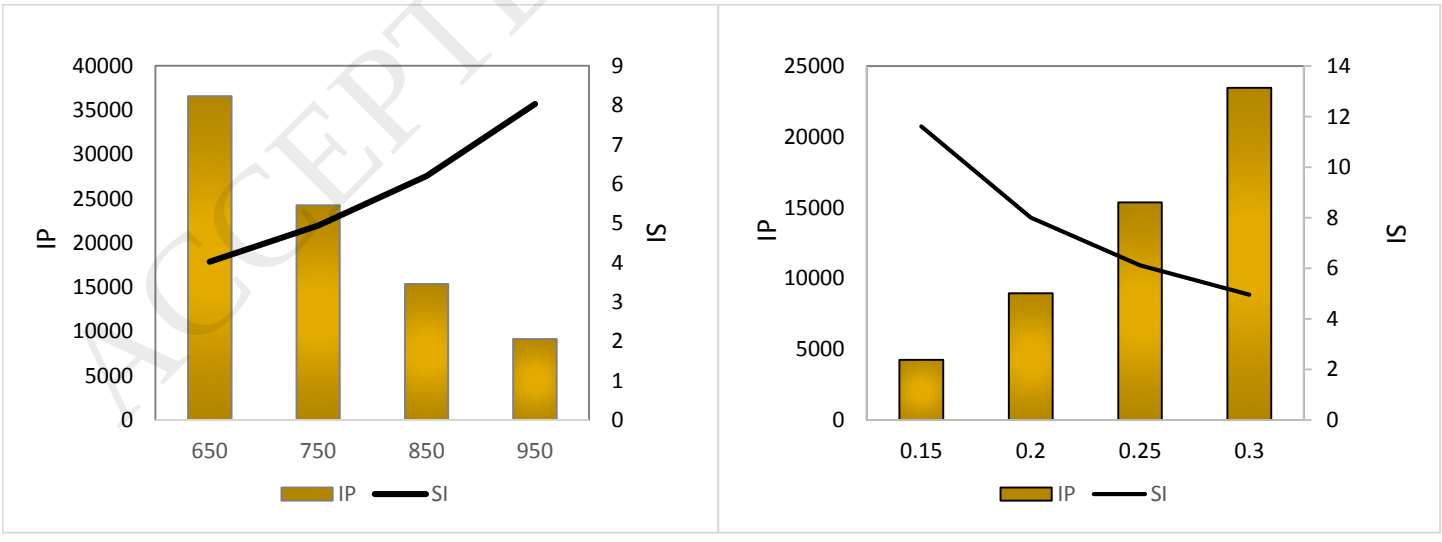

(a) (b)

Figure 4. a) Effect of temperature on the IP and SI of stalk gasification process, b) Effect of ER on the IP and SI of stalk gasification process.

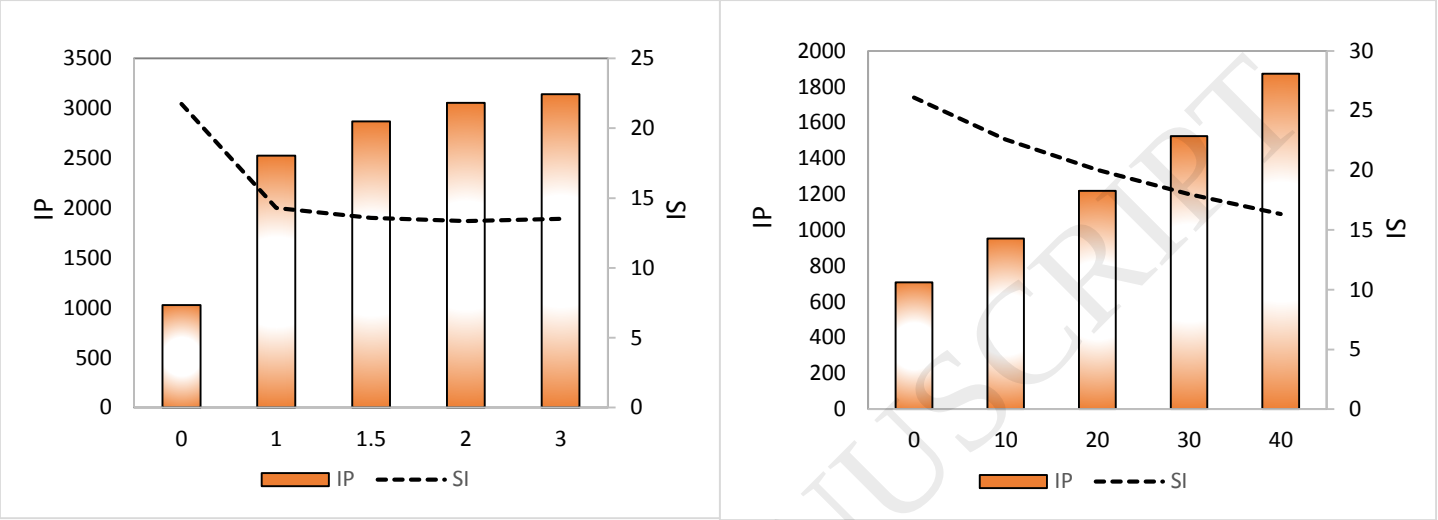

(a) (b)

Figure 5. a) Effect of SBR on the IP and SI of marc gasification process, b) Effect of moisture content on the IP and SI of marc gasification process.

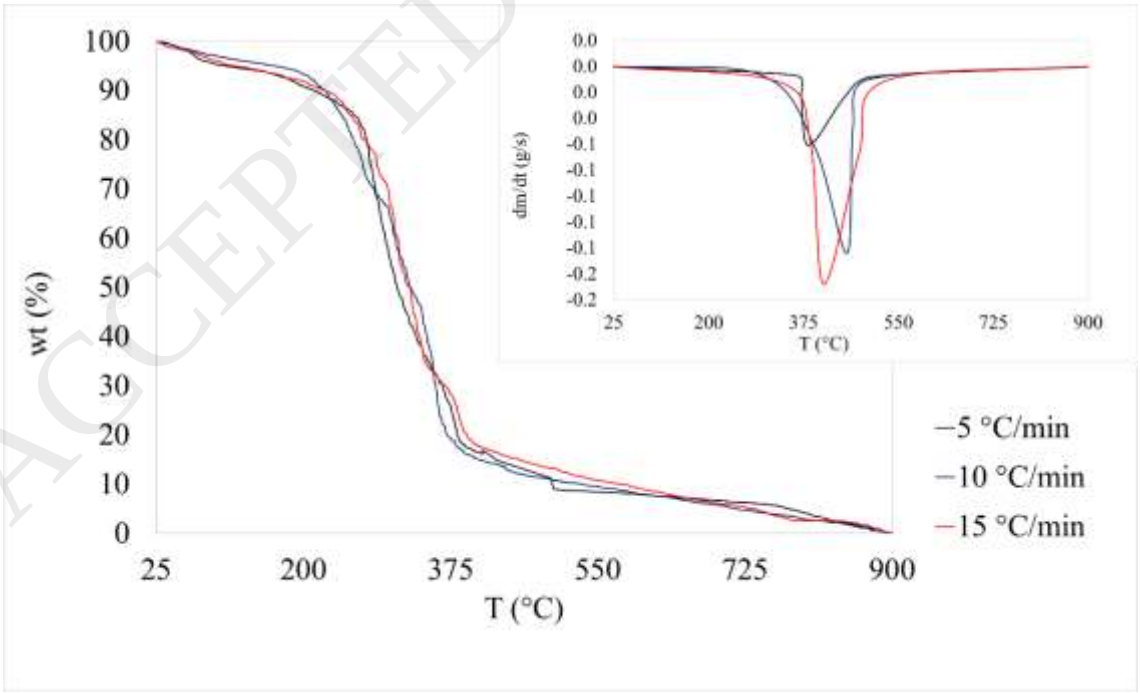

Figure 6. Weight loss and derivatives curves for grape stalk at different heating rates

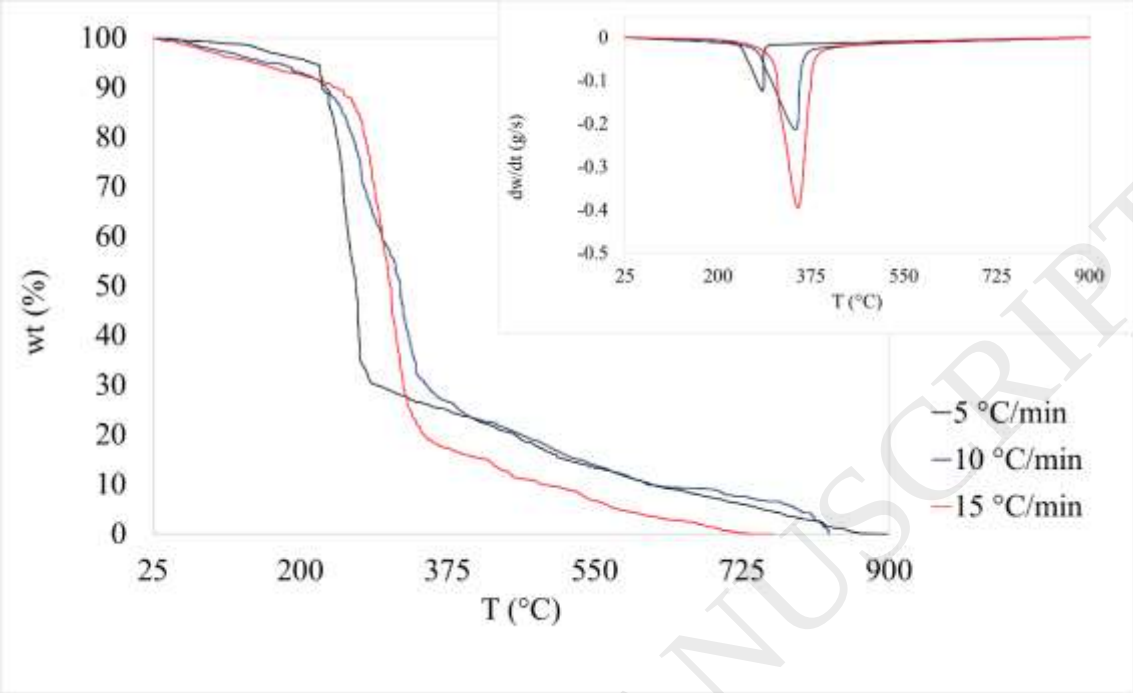

Figure 7. Weight loss and derivatives curves for grape marc at different heating rates

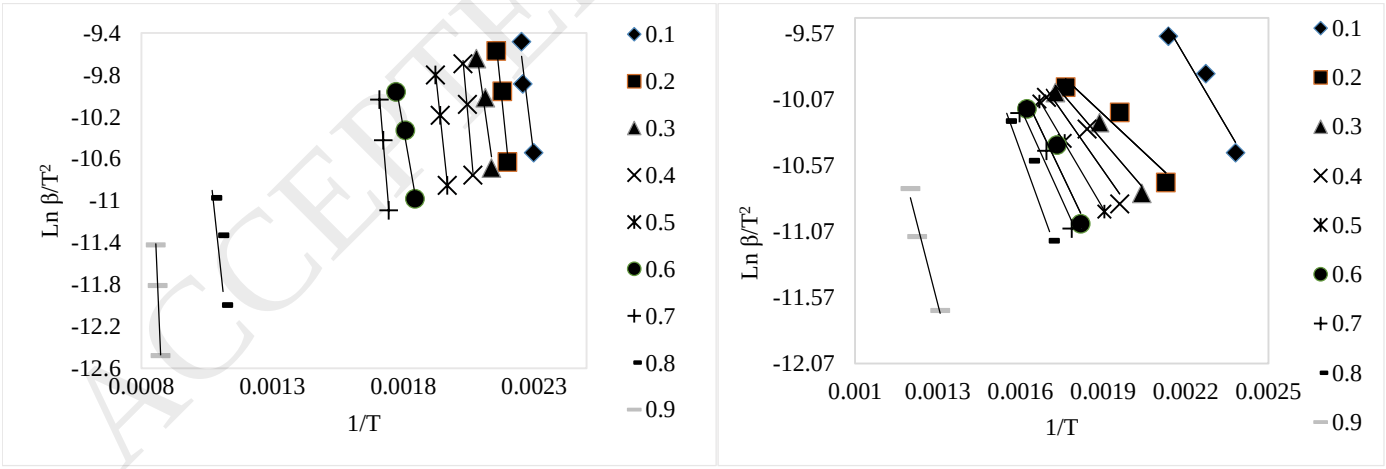

a) b)

Figure 8. Linear regression to conversion range 0.1-0.9 for a) grape stalk and b) grape marc.

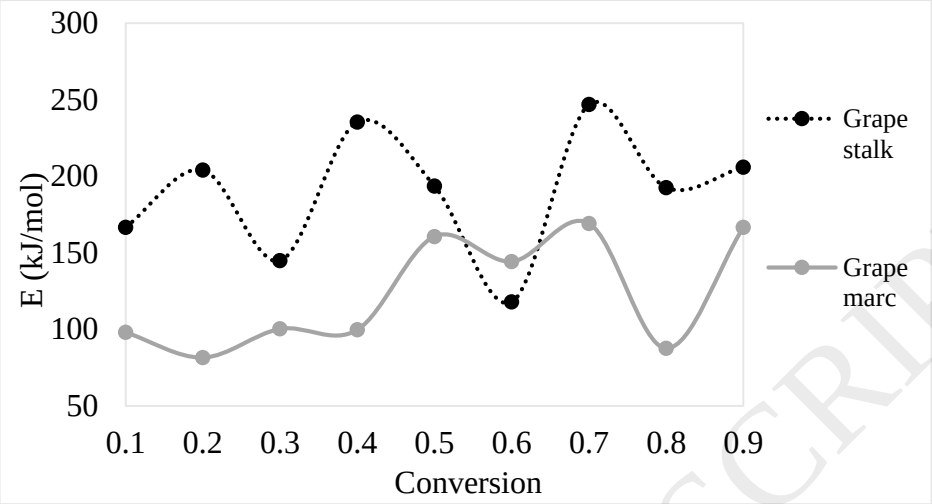

Figure 9. Dependence of the activation energy on the extent of evaluated conversion.

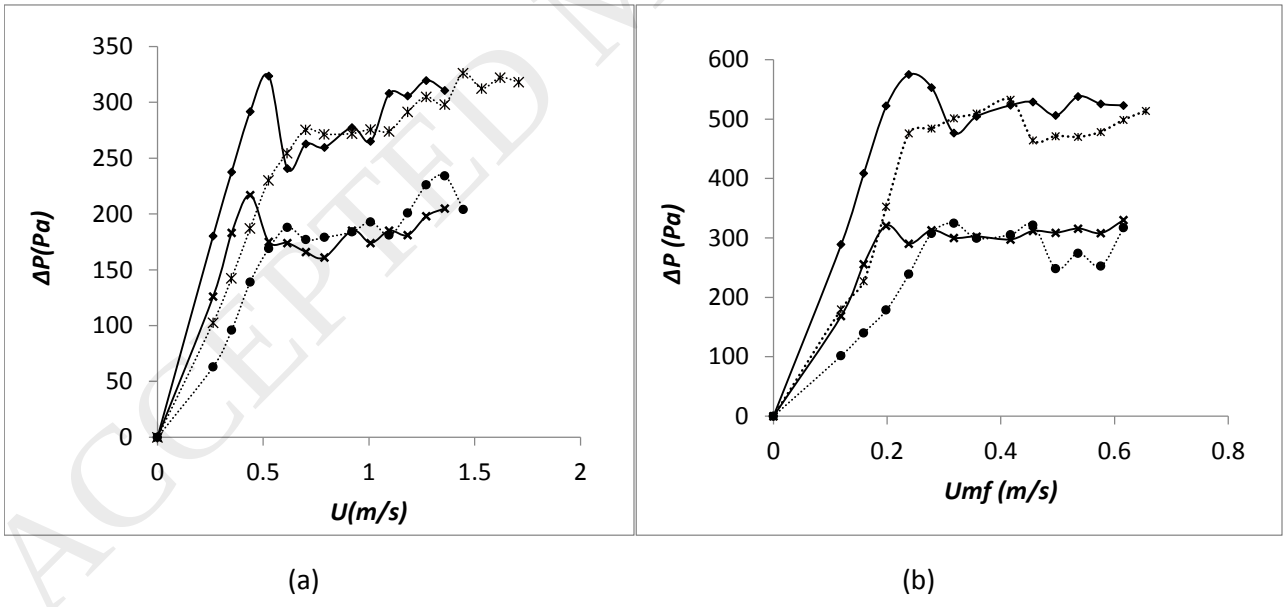

Figure 10. Hydrodynamic curves for: a) pure stalk and b) stalk/sand mixture (…•… decreasing gas velocity, L/D = 0.5, …*… decreasing gas velocity, L/D = 0.75, -x- increasing gas velocity, L/D = 0.5, -♦- increasing gas velocity, L/D = 0.75).

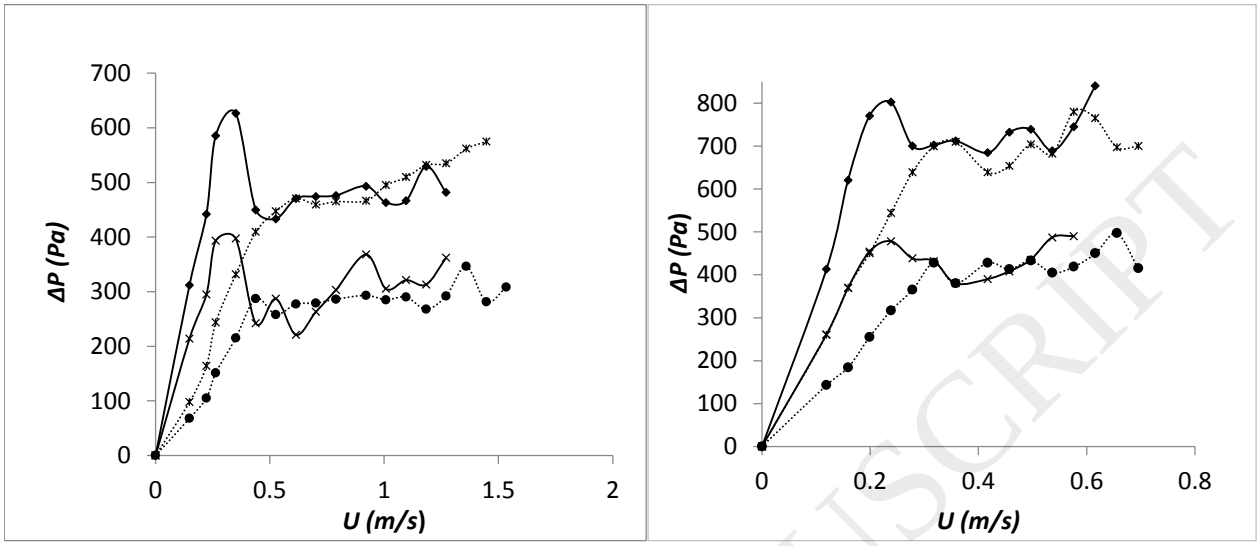

(a) (b)

Figure 11. Hydrodynamic curves for: a) pure marc and b) marc /sand mixture.(…•… decreasing gas velocity, L/D = 0.5, …*… decreasing gas velocity, L/D = 0.75, -x- increasing gas velocity, L/D = 0.5, -♦- increasing gas velocity, L/D = 0.75).

Table

Table 1. Results of Proximate and Ultimate Analysis (Dry Basis, Weight Percentage). High heating values (HHV)

Biomass type	Ultimate analysis (%), dry basis					Proximate analysis (%), dry basis				High heating value HHV (MJ/kg)	Low heating value LHV (MJ/kg)
	C	H	O*	N	S	Moisture	Volatile matter	Fixed carbon	Ash		
Grape stalk	46.14	5.74	37.54	6.37	4.21	7.70	55.84	23.07	10.16	18.34	17.08
Grape marc	52.91	5.93	30.41	5.41	5.34	8.38	68.60	21.98	8.81	20.41	19.11

* By difference

Table 2. Metals contents in the marc and stalks (dry basis)

	Al (mg/kg)	**As (mg/kg)**	**Ba (mg/kg)**	**Ca (mg/kg)**	**Co (mg/ kg)**	**Cu (mg/ kg)**
Marc	26.97±0.02	2.12±0.01	5.11±0.01	165.40±0.10	3.54±0.01	14.86+0.03
Stalk	28.86±0.03	3.65±0.01	5.36±0.02	276.60±0.15	3.57±0.01	17.31±0.02
	In (mg/ kg)	**K (mg/ kg)**	**Li (mg/ kg)**	**Mg (mg/ kg)**	**Na (mg/ kg)**	**P (mg/ kg)**
Marc	8.27±0.02	160.70±0.15	5.76±0.01	48.67±0.03	105.90±0.10	72.26±0.05
Stalk	8.14±0.02	191.90±0.10	5.99±0.02	63.72±0.04	149.10±0.15	63.64±0.05
	Si (mg/ kg)	**Sr (mg/ kg)**	**Tl (mg/ kg)**	**Zn (mg/ kg)**		
Marc	4.04±0.01	0.80±0.01	10.55±0.03	22.36±0.02		
Stalk	4.22±0.01	1.75±0.01	10.38±0.03	24.26±0.02		

Table 3. Contents of lignin, cellulose and hemicellulose determined by ASTM standard methods

	Marc	Stalk
Hemicellulose (%)	4.96±0.01	5.78±0.01
Cellulose (%)	15.31±0.03	16.02±0.02
Lignine (%)	37.97±0.05	30.79±0.04

Table 4. Physical properties characterization and corresponding Geldart classification on behavior of the considered biomass and sand particles

Material		GC	Density	Size	$\bar{D}p$
			(g/cm^3)	mm	mm
Marc		B	1.10±0.005	0.60-1.00	0.81
Stalk		B	0.95±0.003	0.60-1.00	0.87
Inert material of bed		B	2.34±0.3	0.25-0.71	0.33

Table 5. Calculated emission factor of different trace elements for winery wastes

	As (kg/TJ)	In (kg/TJ)	Li (kg/TJ)	Tl (kg/TJ)	Zn (kg/TJ)
Marc	$1.59*10^{-4}$	$1.59*10^{-4}$	$4.33*10^{-4}$	$1.59*10^{-4}$	$1.67*10^{-3}$
Stalk	$3.03*10^{-4}$	$3.03*10^{-4}$	$4.98*10^{-4}$	$3.03*10^{-4}$	$2.07*10^{-3}$

Table 6. Activation energy and pre-exponential factor

Wastes	A	E (kJ/mol)	A (s^{-1})	R^2
Grape stalk	0.1	166.65	$2.91\ 10^{19}$	0.92
	0.2	204.00	$9.06\ 10^{22}$	0.96
	0.3	144.85	$3.52\ 10^{15}$	0.92
	0.4	235.42	$8.51\ 10^{24}$	0.99
	0.5	193.52	$1.95\ 10^{19}$	0.99
	0.6	117.93	$3.18\ 10^{10}$	0.99
	0.7	246.79	$7.82\ 10^{21}$	0.98
	0.8	192.54	$1.32\ 10^{10}$	0.90
	0.9	205.96	$3.30\ 10^{08}$	0.98
	Average	189.74± 41.13	$9.57\ 10^{23}$	
Grape marc	0.1	98.08	$6.90\ 10^{16}$	0.99
	0.2	81.63	$7.01\ 10^{13}$	0.97
	0.3	100.31	$1.42\ 10^{16}$	0.99
	0.4	99.69	$6.94\ 10^{15}$	0.99
	0.5	160.61	$4.36\ 10^{15}$	0.99
	0.6	144.23	$5.42\ 10^{13}$	0.92
	0.7	169.27	$8.09\ 10^{15}$	0.98
	0.8	87.60	$2.17\ 10^{07}$	0.99
	0.9	166.66	$3.39\ 10^{11}$	0.99
	Average	123.10± 34.69	$9.96\ 10^{19}$	

Table 7. Minimum fluidization velocity for marc and stalk at different conditions

Geldart Group	**B**					
Particle	Biomass/Biomass+Sand % vol.	L_{bed}/D_{bed}	x_b	δ (g/cm^3)	$\bar{D}p$ (mm)	$Umf_{exp.i}$ (m/s)
Marc	100	0.5	1	1.10	0.81	0.40
		0.75	1	1.10	0.81	0.44
Stalk		0.5	1	0.95	0.87	0.53
		0.75	1	0.95	0.87	0.56
Marc	75	0.5	0.585	1.41	0.59	0.32
		0.75	0.585	1.41	0.59	0.33
Stalk		0.5	0.549	1.30	0.62	0.27
		0.75	0.549	1.30	0.62	0.30